21

Effect of Ligands on the Photoconductivity of HgTe Nanoplatelets

© P.S. Parfenov[1], Y.V. Grinevich[1], A.V. Sokolova[1], A.A. Babaev[1], I.D. Skurlov[1], S.A. Cherevkov[1], I.E. Kolesnikov[2], A.P. Litvin[1]

[1] Center of Optical Information Technologies, ITMO University, St. Petersburg, Russia
[2] Center for Optical and Laser materials research, St. Petersburg, Russia

e-mail: qrspeter@gmail.com

Received July 18, 2022
Revised August 17, 2022
Accepted August 30, 2022

Near-IR semiconductor colloidal nanoplatelets (NPs) are a new and promising class of materials for the development of photodetectors because they can effectively absorb visible and infrared optical radiation. In this work, we study the photoconductivity of HgTe colloidal nanoplatelets with ligands of 1,2-ethanedithiol and tetrabutylammonium iodide. It has been shown that the choice of ligands is a key factor in achieving high operational characteristics. It has been shown that the photoconductivity sensitivity reaches 0.995 and the specific detectivity reaches $1.2 \cdot 10^9$ J Jones when 1,2-ethadithiol is used as ligands.

Keywords: Near-IR, photodetectors, specific detectivity, EDT, TBAI.

DOI: 10.21883/EOS.2022.11.55111.3871-22

Introduction

The best infrared photodetectors, spectrometers, and imaging arrays are currently produced on the basis of InGaAs, InSb, InAsSb, and HgCdTe single crystals, as well as on epitaxial superlattices. These materials are used for all regions of the IR spectrum: near-IR (SWIR, $1-2.5\,\mu$m), mid-IR (MWIR, $3-5\,\mu$m) and long-wave IR (LWIR, $8-12\,\mu$m) and are used in SWIT thermal imagers for long-range detection, in MWIR thermal imagers for detecting people and animals, and in MWIR spectroscopy for detecting greenhouse gases, pollutants, and crop monitoring [1,2].

Examples of new materials in the IR range are colloidal nanocrystals (NCs) InAs, PbS and PbSe. They gained mainstream attention due to their excellent optical properties, ease of handling, mechanical flexibility and size-adjustable optical absorption range. In recent years, much attention has been paid to colloidal NCs based on mercury telluride (HgTe), with possible absorption from two to tens of microns [1,3], depending on the diameter. As well as to nano-plates (NPls) based on HgTe. The main differences in the optical properties of NPls from NCs are a shorter absorption wavelength (due to stronger confinement), a much narrower photoluminescence band, since the NPls has no inhomogeneous broadening caused by size distribution, and a much shorter fluorescence decay time caused by a large oscillator strength [4] and which is an advantage when creating LEDs. NPls absorption shift further to the NIR can be acheived by doping or growing the CdS layers for example. On the other hand, the absorption band of HgTe NPls is in the more widely studied near-IR range, where detectors can operate without cooling. In addition, NPl sizes can reach several micrometers, which is in demand in the production of photodetectors based on field-effect transistors [5].

HgTe NPls can be used as photoresistors, phototransistors and photodiodes [1,6]. The photodetector device based on photoresistor is the simplest in terms of implementation and description of the operation process. In addition, the photoconductivity underlies the operation of phototransistors. For this reason, the photoconductivity of HgTe NPls was specifically analyzed as a basic study of their electrooptical properties. Among other things, analysis of the photoconductivity can provide information about the behavior of charge carriers in the NPls layer. The choice of ligands is the most important step in the creation of devices based on colloidal NPls and NCs [1]. Hovewer to date, the effect of ligands on the optical and electrical properties of the NP of IR range has practically not been studied. Therefore, in this work, we considered the effect of two types of ligands: 1,2-ethanedithiol (EDT) and tetrabutylammonium iodide (TBAI). These ligands are widely used in solar cells based on PbS/PbSe [7] nanocrystals, therefore a lot of experience in their application has been accumulated. Their short length provides charge carrier transport within nanocrystals layer [8], and they are also one of the main ligands for photodetectors based on nanocrystals for the IR range [9]. EDT is known for providing the best conductivity and is the de facto standard ligand for nanocrystals, while TBAI, being an atomic ligand, provides the smallest distance between nanocrystals and forms a protective layer of iodide on the surface. At the same time, EDT give a good account of oneself in experiments with NC HgTe [10].

Description of the substances under study

HgTe NPls were obtained by total cation-exchange from CdTe NPls. The initial CdTe NPls were synthesized according to the method described in the work [11]. For cation exchange performing anhydrous mercury acetate was

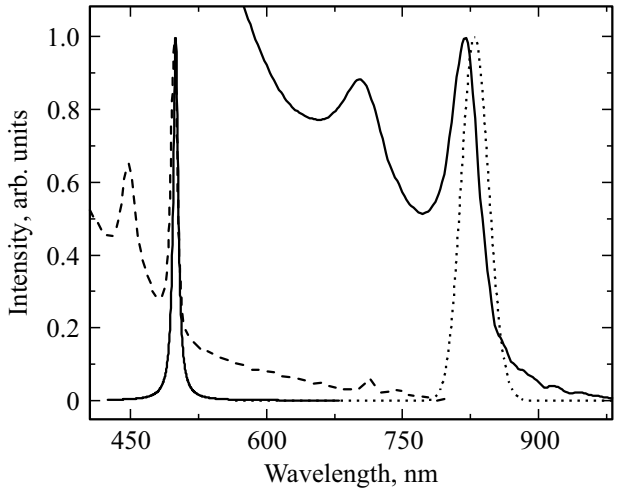

Figure 1. Absorption (solid lines) and photoluminescence (dashed lines) spectra of CdTe NPls (left) and HgTe NPls (right) solutions.

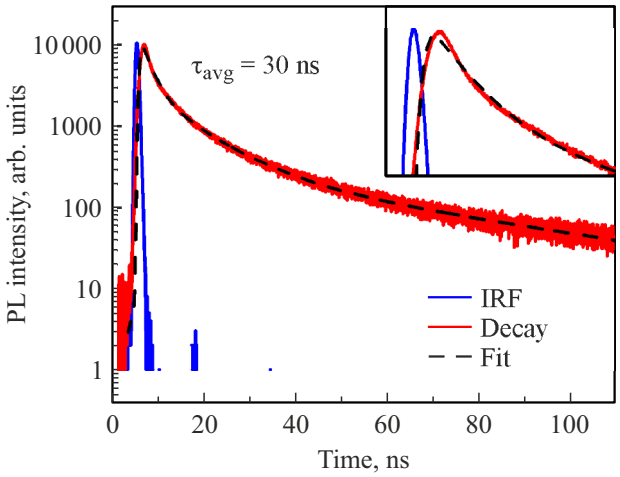

Figure 2. Photoluminescence decay curves of HgTe NPls and approximation by a triexponentially decay function (dashed line).

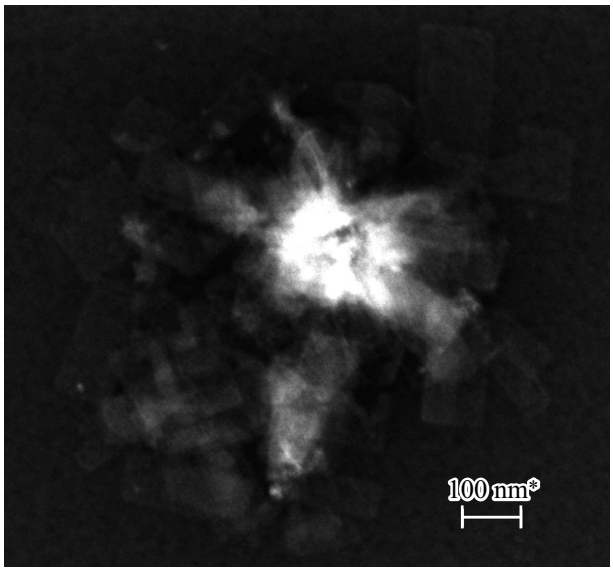

Figure 3. Image of HgTe NPls obtained with a Zeiss Merlin scanning electron microscope. The scale bar is 100 nm. The low contrast is due to the small thickness of the NPls.

dissolved in trioctylamine, and oleic acid was used as a solubilizer. Detailed description of the used cation exchage reaction: 150 μl of the initial solution of CdTe nanoplates are placed in a centrifuge test-tube with further dilution of the solutions with toluene to 15ml. After that, 350 μl of mercury acetate in trioctylamine (concentration 8 mg/ml) is added and the solution is stirred for 18 min. After the completion of the exchange 300 μl of oleic acid is added to the test tube, then the solution is additionally mixed for another 5 min, after which it is centrifuged and the NPls are redissolved in toluene. The absorption and luminescence spectra obtained with a Shimadzu UV-3600 spectrophotometer and a Cary Eclipse spectrofluorimeter are shown in Fig. 1, respectively. On the absorption spectrum of HgTe NPls one can see two local maxima corresponding to two exciton states: „light hole−electron“ (at a wavelength of 700 nm) and „a heavy hole−electron“ (at a wavelength of 820 nm). The luminescence maximum postioned at a wavelength of 830 nm, the band width is 35 nm, which is much smaller than the luminescence band width of IR-range NCs, such as PbS. The photoluminescence decay kinetics (Fig. 2) was measured in the time-correlated single photon counting mode by a Fluorolog-3 spectrofluorimeter (Horiba Jobin Yvon) using a light-emitting diode with a wavelength of 625 nm and a pulse duration of $\sim$ 1 ns. When approximated by a triexponential function, the average decay time was calculated from the formula $\tau_{avg} = \Sigma_i A_i \tau_i^2 / \Sigma_i A_i \tau_i$, where A is amplitude of i-th decay component, τ is decay time of i-th decay component [12]. Hence, averaged PL decay time of HgTe is 30 ns, which agrees with the data given in the work [13] and is much shorter than the times on the order of hundreds of nanoseconds typical for HgTe NCs [14].

According to the electron microscopy results, the dimensions of the HgTe NPls ranged from 100 to 250 nm in length and 50−120 nm in width, an example SEM image is shown in Fig. 3. Judging from the optical properties of the parent CdTe NPls, the thickness of the HgTe NPls is about 2 nm, since the wavelength of the maximum absorption of the „heavy hole-electron“ transition for the CdTe NPls is 500 nm or 2.5 eV, as corresponds to 6 CdTe monolayers or 1.94 nm [11].

Equipment used

The study of photoconductivity was carried out using a Keithley 2636B sourcemeter, Ossila glass substrates with a interdigitated conductive ITO layer previously deposited on them, forming channels 30 mm wide and 50 μm long, and a solar simulator based on a xenon lamp with AM1.5 filter, providing uniform illumination with an intensity of

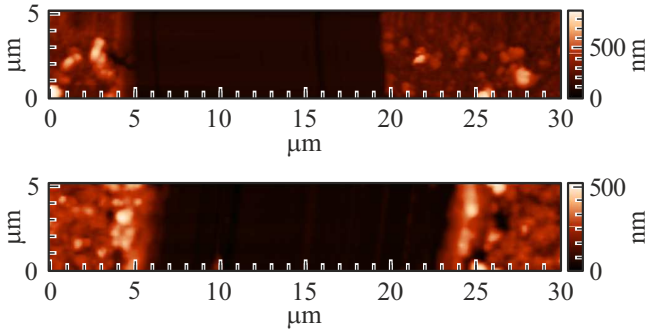

Figure 4. AFM topographic images of HgTe NPls samples with EDT (at top) and TBAI (at bottom) ligands.

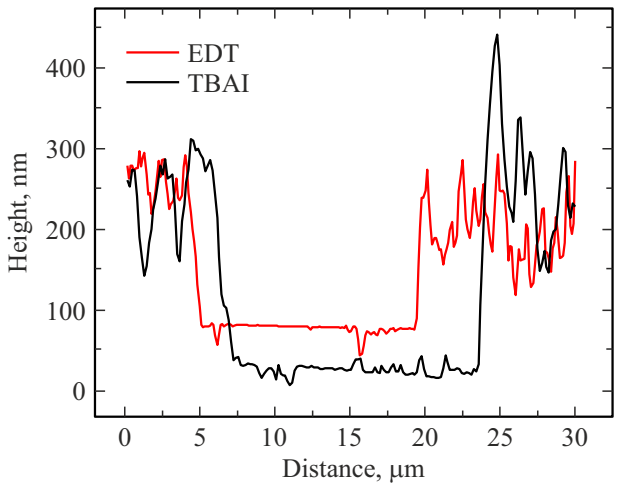

Figure 5. Typical surface profile of HgTe NPls samples with EDT and TBAI ligands obtained using an atomic force microscope.

1000 W/m^2. The layer thickness was estimated using a Solver PRO-M (NT-MDT) atomic force microscope. GN-15-1 helium-neon laser was used as a source of monochromatic radiation, and the lasing output was measured using a Thorlabs PM100D/S130C optical power meter.

Sample preparation

The HgTe NPls films were deposited by spin-coating with subsequent substitution of the initial oleic acid ligands with EDT or TBAI. To do this, the resulting solution of NPls in toluene was deposited on a rotating substrate in a volume of 30 μl at a rotation rate of 2000 min^{-1}. After that, a solution of the corresponding ligands (0.2 vol.% in acetonitrile) was applied to the formed NPls layer for 30 s, after which the sample was spun up to a rate of 2000 min^{-1}. Next, the sample was washed with acetonitrile; it was applied for 30 s, and then the substrate was spun up again. Five depositions were performed to obtain a layer thickness of $\sim$ 150 nm, after which with razor-blade the scratches were made, that is necessary to estimate the layer thickness. Images obtained by atomic force microscope are shown in Fig. 4. Typical scratch-mark profiles on the samples surface are shown in Fig. 5. The thickness of the HgTe NPls samples with EDT ligands was 100–150 nm, and the thickness of the HgTe NPls samples with TBAI ligands was 150–200 nm.

Photoconductivity study

To study the reaction to light, five samples of both types of ligands were studied. The average I-V curves of samples with both types of ligands in the dark and in the light (when illuminated by a sunlight simulator) are shown in Fig. 6 (left). I-V curves are close to linear ones, which indicates the absence of contact resistance or saturation. The average current (at a voltage of 20 V) for samples with EDT ligands in the dark and in the light was 0.6 nA and 113 nA respectively. This reaction to light is more pronounced than in the samples with TBAI ligands: since their average current at a voltage of 20 V was 146 nA and 208 nA in the dark and in the light, respectively.

When comparing the characteristics of detectors, sensitivity (the detector electrical output per unit of radiation energy) is first compared, since its value directly affects the value of the noise-equivalent power (NEP). But the signal must be taken into account without the dark current, which is not related to the optical power. Therefore, to compare samples of different thicknesses, we calculated the specific photoconductivity $\Delta\sigma$, defined as the difference between light and dark specific conductivities σ_L and σ_D:

$$\Delta\sigma = \sigma_L - \sigma_D = \Delta G l/(dh),$$

where ΔG is the difference between the conductivity in the light and in the dark. During calculating the specific conductivity, the layer thickness d was determined using an atomic force microscope and was 125 nm for samples with EDT ligands and 175 nm for samples with TBAI ligands. The layer length l and the width h correspond to the geometry of the substrate electrodes and are 50 μm and 30 mm, respectively. The photoconductive sensitivity, defined by the formula $S = (I_L - I_D)/I_L$, is also calculated. The calculation results are given in the table.

Calculations demonstrate high photosensitivity in the case of EDT and low photosensitivity in the case of TBAI both in absolute change in conductivity and in relative change in current. The reason seems to be that in the case of NPls passivation by EDT molecules, a significant number of defect states can form on the NPls surface. Their appearance is caused by the oxidation of EDT itself and subsequent oxidation of metal atoms [15]. These defect states reduce the conductivity, but under exposure to light the release of trapped charge carriers is accelerated and the conductivity increases significantly. In the case of TBAI, the conductivity is higher, the number of defects is smaller, and therefore the number of light-activated states and the overall response to light are less (a similar phenomenon was observed in the case of PbS NCs in [16]).

To study the stability of the samples, the measurements were additionally carried out after 9 days of storage in

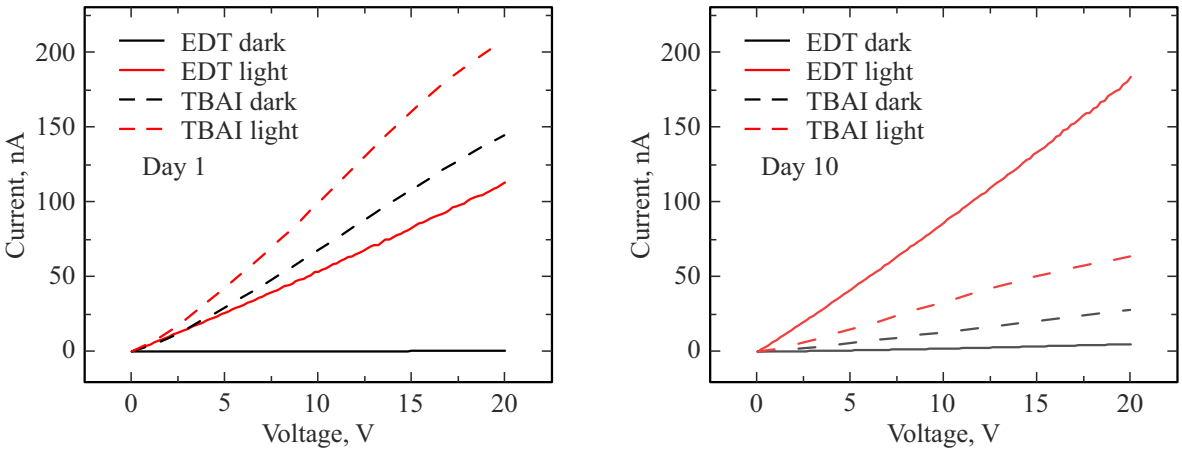

Figure 6. Averaged I–V curves of samples with EDT and TBAI ligands in the dark and under illumination on the 1st day (left) and on the 10th day (right).

Characteristics of HgTe NPls samples with EDT and TBAI ligands

Type Of ligands	Specific dark conductivity		Specific photoconductivity		Sensitivity of photoconductivity	
	σ_0, μS/cm		$\Delta\sigma$, μS/cm		S	
	Day 1	Day 10	Day 1	Day 10	Day 1	Day 10
EDT	0.004	0.34	0.75	0.86	0.995	0.972
TBAI	0.69	0.13	0.3	0.17	0.393	0.560

an inert atmosphere (the measurements themselves were carried out in an ambient air). The results are shown in Fig. 6 (right) and in the table. For HgTe-EDT samples, the dark current increased by two orders of magnitude, and the light current increased by one and a half times. As a result, the relative parameter (the photoconductive sensitivity) slightly decreased, but the absolute parameter (photoconductivity) increased. For the HgTe-TBAI samples, the light and dark currents decreased by a factor of ~ 4. As a result, the photoconductive sensitivity slightly increased. But a more important parameter such as the increase in conductivity decreased almost by a half. Therefore, limited exposure in an ambient air can improve the sensitivity of similar detectors using EDT ligands.

Measurement of spectral sensitivity and specific detectivity

Since the sample with EDT ligands has better photoconductivity and photoconductive sensitivity, we estimated its spectral sensitivity by He-Ne laser (LGN-15-1 with wavelength of 633 nm and output of 15 mW). Laser radiation has an advantage over conventional sources (incandescent lamps, gas discharge lamps and LEDs), since it almost does not require focusing (we have used only the expansion of the beam) and it allows to avoid errors associated with the selection of the desired spectrum estimate by the beam expander, the desired part of the spectrum and with an incorrect estimate of the geometry of the path of the rays. Absorption at wavelength of 633 nm differs from that of in the local maximum at wavelength of 820 nm by only 15%, which makes it possible to obtain trustworthy results with appropriate correction. At an average output of 1.9 μW falling on the active pixel surface (with an area of 1.5 mm^2) and at a voltage of 20 V, the average current was 23.7 nA.

The spectral sensitivity $R_\lambda = I/\mathrm{W}$ at wavelength of 633 nm was 11 mA/W (at 20 V), and the specific detectivity $D^* = R_\lambda\sqrt{(S/(2qI_D)}$ (where q is electron charge, S — detector area, I_D is dark current measured above [13]), used to compare the sensitivity of devices regardless of their area, was $1.1 \cdot 10^9$ J, or, taking into account the difference in spectral sensitivity at wavelength of 633 nm and at absorption peak, 12 mA/W and $1.2 \cdot 10^9$ J.

These values are comparable to IR detectors based on PbS NCs given in [17], where they are $R = 7$ mA/W at 10 V and $D^* \sim 1.7 \cdot 10^9$ J. In comparison with similar photoresistive sensors based on HgTe NPls, the parameters of which are given in [1], it can be seen that the spectral sensitivity is lower, but due to the low dark current, the specific detectivity is approximately at the same level. Further improvement of the photodetector parameters is possible, first of all, by optimizing the technology for forming a thin film from NPls, since the quality of a detector based on colloidal NCs/NPls is largely determined by the

quality of the layer. In addition, such types of detectors are still at the initial development stage, and the performance gap between them and photodetectors of other types (for example, those given in the work [18]) has yet to be overcome.

Conclusion

In this work, the photoconductivity of HgTe NPls samples (obtained by cation exchange from CdTe NPls) with EDT and TBAI ligands was studied. It is shown that the photosensitivity of NPls layers with EDT ligands is much higher, which is explained by the large number of defect states and the release of trapped charge carriers under light exposure. The spectral sensitivity and specific detectivity are calculated, and the obtained results demonstrate a significant potential for the use of HgTe NPls for photodetection.

Funding

This study was financially supported by the Russian Science Foundation (project № 19-13-00332). № 19-13-00332-P). I.D. Skurlov thanks the Russian Foundation for Basic Research (project № 20-32-90208) for the support. Photoluminescence decay kinetics was measured at the Center for optical and laser materials research under financial support of St Petersburg University (project № 93021679).

Conflict of interest

The authors declare that they have no conflict of interest.

References

[1] S. Zhang, Y. Hu, Q. Hao. Coatings, **10** (8), 760 (2020). DOI: 10.3390/coatings10080760
[2] P. Guyot-Sionnest, M.M. Ackerman, X. Tang. J. Chemical Physics, **151** (6), 060901 (2019). DOI: 10.1063/1.5115501
[3] N. Goubet, A. Jagtap, C. Livache, B. Martinez, H. Portalés, X.Z. Xu, R. Lobo, B. Dubertret, E. Lhuillier. J. Am. Chem. Soc., **140** (15), 5033 (2018). DOI: 10.1021/jacs.8b02039
[4] A. C. Berends, C. de M. Donega. J. Physical Chemistry Letters, **8** (17), 4077 (2017). DOI: 10.1021/acs.jpclett.7b01640
[5] C. Gréboval, E. Izquierdo, C. Livache, B. Martinez, M. Dufour, N. Goubet, N. Moghaddam, J. Qu, A. Chu, J. Ramade, H. Aubin, H. Cruguel, M. Silly, E. Lhuillier, S. Ithurria. Nanoscale, **11** (9), 3905 (2019). DOI: 10.1039/C8NR09644A
[6] C. Livache, E. Izquierdo, B. Martinez, M. Dufour, D. Pierucci, S. Keuleyan, H. Cruguel, L. Becerra, J.L. Fave, H. Aubin, A. Ouerghi, E. Lacaze, M.G. Silly, B. Dubertret, S. Ithurria, E. Lhuillier. Nano Letters, **17** (7), 4067 (2017). DOI: 10.1021/acs.nanolett.7b00683
[7] A. Babaev, P. Parfenov, D. Onishchuk, A. Dubavik, S. Cherevkov, A. Rybin, M. Baranov, A. Baranov, A. Litvin, A. Fedorov, Materials, **12** (24), 4221 (2019). DOI: 10.3390/ma12244221
[8] S. Ahn, C. Ingrosso, A. Panniello, M. Striccoli, G.V. Bianco, A. Agostiano, G. Bruno, M. L. Curri, O. Vazquez-Mena. Adv. Electron. Mater., **8**, 2100672 (2022). DOI: 10.1002/aelm.202100672
[9] S.B. Hafiz, M.M. Al Mahfuz, M.R. Scimeca, S. Lee, S.J. Oh, A. Sahu, D.-K. Ko. Phys. E: Low-Dimens. Syst. Nanostruct., **124**, 114223 (2020). DOI: 10.1016/j.physe.2020.114223.
[10] M. Chen, X Lan, X. Tang, Y. Wang, M.H. Hudson, D.V. Talapin, P. Guyot-Sionnest. ACS Photonics, **6** (9), 2358 (2019). DOI: 10.1021/acsphotonics.9b01050
[11] S. Ithurria, M.D. Tessier, B. Mahler, R.P.S.M. Lobo, B. Dubertret, Al.L. Efros. Nature Materials, **10** (12), 936 (2011). DOI: 10.1038/nmat3145
[12] J.R. Lakowicz. *Principles of fluorescence spectroscopy* (Springer, Boston, MA, 1999), ch. 4. DOI: 10.1007/978-1-4757-3061-6_4
[13] P. Geiregat, A.J. Houtepen, L.K. Sagar, I. Infante, F. Zapata, V. Grigel, G. Allan, C. Delerue, D.V. Thourhout, Z. Hens. Nature Materials, **17**—,(1), 35 (2018). DOI: 10.1038/nmat5000
[14] E. Izquierdo, A. Robin, S. Keuleyan, N. Lequeux, E. Lhuillier, S. Ithurria. J. Am. Chem. Soc., **138** (33), 10496 (2016). DOI: 10.1021/jacs.6b04429
[15] J.M. Luther, M. Law, Q. Song, C.L. Perkins, M.C. Beard, A.J. Nozik. ACS Nano, **2** (2), 271 (2008). DOI: 10.1021/nn7003348
[16] P.S. Parfenov, N.V. Bukhryakov, D.A. Onishchuk, A.A. Babaev, A.V. Sokolova, A.P. Litvin. FTP, **56** (2), 236 (2022) (in Russian). DOI: 10.21883/FTP.2022.02.51968.9734
[17] A. Maulu, J. Navarro-Arenas, P.J. Rodríguez-Cantó, J.F. Sánchez-Royo, R. Abargues, I. Suárez, J.P. Martínez-Pastor. Nanomaterials, **8** (9), 677 2018). DOI: 10.3390/nano8090677
[18] D. Yang, D. Ma. Advanced Optical Materials, **7** (1), 1800522 (2019). DOI: 10.1002/adom.201800522